AGU PUBLICATIONS

JGR

Journal of Geophysical Research: Atmospheres

RESEARCH ARTICLE
10.1002/2016JD025305

Key Points:
- Regional circulation anomalies associated with the SAM dominate temporal temperature variability on the Antarctic Peninsula during summer and autumn
- ENSO-Peninsula temperature relationship is strongest on the western Peninsula but statistically significant only during winter and spring
- Northeast Peninsula temperatures are dominated by SAM-related zonal flow and leeside Föhn effects during all seasons

Correspondence to:
K. R. Clem,
kyle.clem@vuw.ac.nz

Citation:
Clem, K. R., J. A. Renwick, J. McGregor, and R. L. Fogt (2016), The relative influence of ENSO and SAM on Antarctic Peninsula climate, *J. Geophys. Res. Atmos.*, *121*, 9324–9341, doi:10.1002/2016JD025305.

Received 2 MAY 2016
Accepted 28 JUL 2016
Accepted article online 1 AUG 2016
Published online 22 AUG 2016

The relative influence of ENSO and SAM on Antarctic Peninsula climate

Kyle R. Clem[1], James A. Renwick[1], James McGregor[1], and Ryan L. Fogt[2]

[1]School of Geography, Environment and Earth Sciences, Victoria University of Wellington, Wellington, New Zealand, [2]Department of Geography, Ohio University, Athens, Ohio, USA

Abstract Recent warming of the Antarctic Peninsula during austral autumn, winter, and spring has been linked to sea surface temperature (SST) trends in the tropical Pacific and tropical Atlantic, while warming of the northeast Peninsula during summer has been linked to a strengthening of westerly winds traversing the Peninsula associated with a positive trend in the Southern Annular Mode (SAM). Here we demonstrate that circulation changes associated with the SAM dominate interannual temperature variability across the entire Antarctic Peninsula during both summer and autumn, while relationships with tropical Pacific SST variability associated with the El Niño–Southern Oscillation (ENSO) are strongest and statistically significant primarily during winter and spring only. We find the ENSO-Peninsula temperature relationship during autumn to be weak on interannual time scales and regional circulation anomalies associated with the SAM more important for interannual temperature variability across the Peninsula during autumn. Consistent with previous studies, western Peninsula temperatures during autumn, winter, and spring are closely tied to changes in the Amundsen Sea Low (ASL) and associated meridional wind anomalies. The interannual variability of ASL depth is most strongly correlated with the SAM index during autumn, while the ENSO relationship is strongest during winter and spring. Investigation of western and northeast Peninsula temperatures separately reveals that interannual variability of northeast Peninsula temperatures is primarily sensitive to zonal wind anomalies crossing the Peninsula and resultant leeside adiabatic warming rather than to meridional wind anomalies, which is closely tied to variability in the zonal portion of the SAM pattern.

1. Introduction

The Antarctic Peninsula consists of a steep mountain range (~2000 m in elevation) that extends equatorward from the high West Antarctic Ice Sheet plateau. The Bellingshausen and Weddell Seas surround the Peninsula to its west and east, respectively, and the Drake Passage off its northern tip. There are three primary processes that drive temperature variability across the Peninsula: meridional temperature advection associated with regional circulation [*Ding and Steig*, 2013; *Clem and Fogt*, 2013; *Clem and Renwick*, 2015], orographic effects from westerly winds interacting with the mountainous terrain including leeside Föhn effects on the eastern Peninsula and low-level blocking on the western side [*Orr et al*., 2004, 2008], and the sea ice distribution in its surrounding seas [*Turner et al*., 2013a].

Studies have identified significant climate change across the Antarctic Peninsula since the midtwentieth century, but the observed changes are not uniform across the Peninsula in space or time. Significant warming trends have been documented along the western Antarctic Peninsula since the mid-1950s [*King*, 1994; *Vaughan et al*., 2001, 2003; *Turner et al*., 2005; *Clem and Fogt*, 2015]. The western Peninsula warming is strongest during the austral autumn and winter seasons and has been linked to reductions in sea ice off the west coast of the Peninsula [*Meredith and King*, 2005; *Ding and Steig*, 2013]. Recent studies have also shown significant warming of the western Peninsula during spring, which has persisted over recent decades, while the warming trends during autumn and winter have weakened slightly [*Clem and Fogt*, 2015]. The spring warming on the western Peninsula has been linked to strengthened northerly flow from increased pressures in the South Atlantic and also persistent negative sea ice anomalies off the western coast due to decreases in the preceding autumn and winter seasons [*Ding and Steig*, 2013; *Clem and Fogt*, 2015; *Clem and Renwick*, 2015]. The warming and reduced sea ice along the western Peninsula have had major biological impacts, including an increase in competition for krill-eating predators due to reductions in sea ice [*Trivelpiece et al*., 2011] and the ability for king crab populations to survive at unprecedented shallow depths along the outer shelf of the western Antarctic Peninsula [*Aronson et al*., 2015].

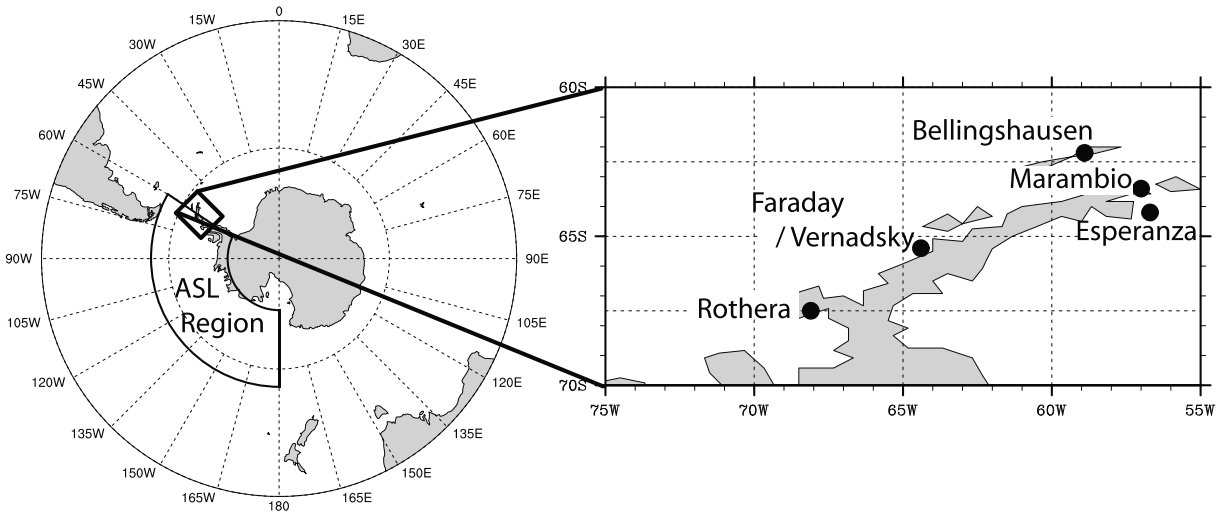

Figure 1. Map of study area showing Antarctic Peninsula stations and ASL region.

Significant warming has also been observed across the northeastern Peninsula since the mid-1950s [*Skvarca et al*., 1998; *Turner et al*., 2005; *Orr et al*., 2008], namely, at Esperanza and Marambio stations (see Figure 1 for stations), although the rate of warming here has also decreased slightly in recent decades [*Clem and Fogt*, 2015]. In contrast to the winter and spring warming of the western Peninsula, the northeast Peninsula exhibits the strongest warming trend during summer, which has been linked to a strengthening of the circumpolar westerlies associated with a positive trend in the Southern Annular Mode (SAM) [*Marshall et al*., 2006; *Orr et al*., 2008]. Closely linked to the northeast Peninsula warming has been the collapse of northern portions of the Larsen Ice Shelf located on the eastern Peninsula and the rapid acceleration and thinning of glaciers flowing into the collapsed ice shelves [*Fahnestock et al*., 2002; *Scambos et al*., 2004]. Satellite images revealed that surface melting in response to warming near-surface air temperatures was the dominant process leading to the disintegration and collapse of the ice shelves [*Vaughan and Doake*, 1996; *Scambos et al*., 2000; *Fahnestock et al*., 2002], indicating that the Peninsula's ice shelves and interior glaciers are highly sensitive to local climate changes.

To the west of the Peninsula in the Bellingshausen and Amundsen Seas lies a semipermanent climatological low pressure termed the Amundsen Sea Low (ASL; see Figure 1 for the ASL region) [*Fogt et al*., 2012a; *Turner et al*., 2013b]. The ASL is the dominant regional atmospheric circulation feature in the vicinity of the Peninsula, and it exists due to a combination of local topography [*Lachlan-Cope et al*., 2001] and persistent cyclonic activity across the region [*Baines and Fraedrich*, 1989; *Walsh et al*., 2000; *Fogt et al*., 2012a]. The ASL strength and position dominate regional climate and sea ice variability across West Antarctica and the Antarctic Peninsula through modification of local meridional winds [*Lefebvre et al*., 2004; *Stammerjohn et al*., 2008; *Hosking et al*., 2013; *Clem and Fogt*, 2013; *Turner et al*., 2015].

Variability in the ASL is related to hemispheric-wide pressure fluctuations manifested in the SAM as well as remote forcing from the tropical Pacific and tropical Atlantic Oceans. The SAM, which represents a seesaw in atmospheric mass between the Southern Hemisphere middle latitudes (~40°S) and the polar cap (poleward of ~65°S), has been shown to significantly modulate ASL intensity. When the SAM is in its positive phase, below normal pressure is observed over the high southern latitudes and the storm track intensifies/shifts poleward toward the Antarctic continent [*Thompson et al*., 2000]. The ASL tends to be stronger than normal during positive SAM conditions, which amplifies local meridional wind anomalies and brings stronger northerly winds to the western Peninsula [*Fogt et al*., 2011, 2012a; *Turner et al*., 2013b; *Hosking et al*., 2013]. The SAM has been shown to influence the northeastern Peninsula climate in a different fashion. When the SAM is in its positive phase, particularly during summer, strengthened westerly winds flow over the Peninsula leading to leeside adiabatic warming on the eastern Peninsula [*Orr et al*., 2008].

Sea surface temperature (SST) anomalies in the tropical Pacific and tropical Atlantic basins also influence ASL intensity and the nearby Peninsula climate. Positive SST anomalies in the western tropical Pacific associated with the La Niña phase of the El Niño–Southern Oscillation (ENSO) have been shown to deepen and broaden the ASL, while El Niño conditions tend to weaken the ASL [*Fogt et al*., 2011, 2012a; *Turner et al*., 2013b; *Clem and Fogt*, 2013]. Recent studies have also shown that positive SST anomalies in the tropical North Atlantic can strengthen the ASL during the winter and spring seasons [*Li et al*., 2014; *Simpkins et al*., 2014]. As with forcing from the SAM, when the ASL is intensified through tropically forced Rossby waves, the northerly flow to the Peninsula is strengthened leading to warming and reductions in sea ice along the west coast of the Peninsula.

Given the dramatic changes that have occurred across the Peninsula over recent decades, including the collapse of ice shelves, acceleration and thinning of glaciers, and major ecological and biological shifts, it is important to understand in detail the mechanisms that drive climate variability in this region. *Ding and Steig* [2013] showed that warming of the entire Antarctic Peninsula during autumn, winter, and spring was related to tropical Pacific forcing during autumn that deepened the ASL and reduced sea ice along the western Peninsula coast. However, *Clem and Fogt* [2013] showed that during spring, the impact of the tropical Pacific on Peninsula climate is variable in space and time, and relationships with ENSO were only temporally persistent and significant on the western Peninsula, while atmospheric circulation anomalies associated with the SAM dominated climate variability on the northeast Peninsula. Therefore, *Ding and Steig* [2013] may have overlooked the role of the SAM at modulating climate variability on the Peninsula by investigating western and northeast Peninsula temperatures as a single quantity. In this study, we explore the relative roles of atmospheric circulation anomalies associated with ENSO and SAM phases on Peninsula climate by investigating the western and northeast Peninsula separately. This study builds upon the work of *Ding and Steig* [2013] by taking into consideration the findings of *Clem and Fogt* [2013] and investigating the spatial impacts of tropical and SAM forcing on Antarctic Peninsula climate during all seasons. The paper is laid out as follows: section 2 provides an overview of the data and methods used for the study, section 3 contains results, and a discussion and conclusions are offered in section 4.

2. Data and Methods

Atmospheric data are from the European Centre for Medium-Range Weather Forecasts (ECMWF) Interim Reanalysis (ERA-Interim) [*Dee et al*., 2011] employed at 1.5° × 1.5° resolution starting in 1979. Results using ERA-Interim were compared with the National Aeronautic and Space Administration Modern-Era Retrospective Analysis for Research and Applications version 2 (MERRA-2) [*Rienecker et al*., 2011] as well as other spatial resolutions of ERA-Interim. Similar results were obtained in all cases. Because of ERA-Interim's superior performance at tropospheric levels over the high southern latitudes, particularly with tropospheric winds over the Amundsen and Bellingshausen Seas, only results using ERA-Interim are shown [*Bromwich et al*., 2011; *Bracegirdle and Marshall*, 2012; *Bracegirdle*, 2012]. Sea surface temperature data are from the Met Office Hadley Centre's sea ice and sea surface temperature data set (HadISST) [*Rayner et al*., 2003] employed at 1° × 1° resolution, also starting in 1979. Results obtained using HadISST were compared with National Oceanic and Atmospheric Administration (NOAA) Extended Reconstructed SST version 4 data [*Huang et al*., 2014; *Liu et al*., 2014], and similar results were obtained.

El Niño–Southern Oscillation (ENSO) activity is monitored using the Southern Oscillation Index (SOI) and sea surface temperature anomalies in the Niño 3.4 region (5°N–5°S, 170°W–120°W), both accessed online from the Climate Prediction Center (www.cpc.ncep.noaa.gov/data/indices). The SAM is monitored using the observation-based index of *Marshall* [2003], accessed online at legacy.bas.ac.uk/met/gjma/sam.html. Antarctic Peninsula meteorological data are from the quality-controlled Reference Antarctic Data for Environmental Research archive [*Turner et al*., 2004]. Five stations (Figure 1) with the most complete temperature records spanning 1979–2015 are used for this study. Variability in the Amundsen Sea Low (ASL) is monitored following *Fogt et al*. [2012a] using the ERA-Interim monthly minimum sea level pressure value in the region 55–75°S, 180–60°W (Figure 1).

The ENSO and SAM relationship with Antarctic Peninsula temperatures is investigated using linear correlation and anomaly composites. All correlations are calculated on detrended data, while years used for Peninsula temperature composites are selected using the original (nondetrended) data. The statistical significance of correlations and anomalies is calculated following a two-tailed Student's *t* test against the null hypothesis

Table 1. Seasonal Detrended Correlations of Antarctic Peninsula Temperatures with the SOI, Niño 3.4 SST Anomalies, and *Marshall* [2003] SAM Index Over 1979–2015[a]

	DJF			MAM			JJA			SON		
	SOI	Niño 3.4	SAM	SOI	Niño 3.4	SAM	SOI	Niño 3.4	SAM	SOI	Niño 3.4	SAM
All Peninsula	0.12	−0.14	0.24	0.14	−0.17	**0.67***	0.26	**−0.43***	**0.37**	**0.49***	**−0.49***	**0.51***
West	−0.01	−0.07	**−0.31**	**0.33**	**−0.31**	**0.50***	**0.39**	**−0.55***	0.16	**0.59***	**−0.59***	**0.30**
Northeast	0.12	−0.10	**0.45***	0.01	−0.07	**0.61***	0.12	**−0.28**	**0.44***	**0.33**	**−0.32**	**0.56***
ASL	**−0.35**	**0.35**	**−0.78***	**−0.28**	0.09	**−0.50***	**−0.29**	**0.33**	**−0.72***	−0.18	0.20	**−0.81***

[a]All Peninsula temperatures are the average of the five stations shown in Figure 1: Rothera, Faraday, Bellingshausen, Marambio, and Esperanza. Western Peninsula temperature is the average of Rothera and Faraday, and northeast Peninsula temperature is the average of Esperanza and Marambio. Also given are the detrended correlations with ASL magnitude, which is the minimum sea level pressure value in the region 55–75°S, 180–60°W. The boldface correlations are significant at $p < 0.10$, boldface and underlined correlations are significant at $p < 0.05$, and correlations significant at $p < 0.01$ are denoted with an asterisk.

of a zero correlation and a zero anomaly, respectively. Anomalies are calculated from the 1981–2010 climatological base period. Seasonal means are with respect to the Southern Hemisphere: summer is December-January-February (DJF), autumn is March-April-May (MAM), winter is June-July-August (JJA), and spring is September-October-November (SON). Summer refers to the December year. The period of study is 1979–2015.

3. Results

3.1. Seasonal and Spatial Influence of ENSO and SAM on Antarctic Peninsula Temperatures

Seasonal detrended correlations of Antarctic Peninsula temperatures with the SOI, Niño 3.4 SST anomalies, and the Marshall SAM index over 1979–2015 are given in Table 1. To investigate the spatial relationship of ENSO and SAM with Peninsula temperatures (following *Clem and Fogt* [2013]), the average temperature for Faraday-Vernadsky and Rothera stations (hereafter western Peninsula) and Marambio and Esperanza stations (hereafter northeast Peninsula) are analyzed separately from the full five-station average that represents Peninsula-wide temperatures (see Figure 1 for all stations and location of western and northeast Peninsula stations). Bellingshausen station, situated on the northern Peninsula, is included only in the "all Peninsula" mean because it lies between the western and northeast Peninsula stations, and the local topography is markedly different compared to the western and northeast stations, and therefore has slightly different temperature-wind relationships, as also noted in *Clem and Fogt* [2013].

During DJF, both the ENSO and SAM index correlations with Peninsula-wide temperatures are weak and insignificant. The ENSO relationship is near zero for both the western and northeast regions, consistent with *Ding and Steig* [2013]; however, there are significant, opposing relationships between the SAM and western and northeast Peninsula temperatures. Positive SAM conditions are associated with warming on the northeast Peninsula during DJF (consistent with *Orr et al*. [2008]) but cooling on the western Peninsula. Therefore, the weak, insignificant SAM index correlation with Peninsula-wide temperatures during DJF is misleading as significant SAM relationships exist for both the western and northeast Peninsula but are of opposite sign. The reason for this opposing relationship will be discussed later. During MAM, when *Ding and Steig* [2013] showed a significant relationship between Peninsula-wide temperatures and tropical Pacific SSTs, there is no significant relationship on interannual time scales between ENSO and Peninsula temperatures except for the western Peninsula; even so these correlations are weak and only significant at $p < 0.10$. Instead, much stronger relationships exist between Peninsula temperatures and the SAM index during MAM. The Peninsula-wide relationship with ENSO becomes stronger during JJA and SON, although the ENSO correlation is consistently strongest along the western Peninsula, while the SAM index correlation is strongest with northeast Peninsula temperatures during all seasons.

Partial correlations are given in Table 2, calculated after linearly removing the effect of the SAM index upon the SOI and vice versa. The SOI partial correlation with Peninsula temperatures (and ASL magnitude) during MAM is even weaker after influences of the SAM index are removed, indicating that the original ENSO correlations during MAM (Table 1), albeit weak, are partially a manifestation of covariability with the SAM index. Meanwhile, the SAM index partial correlations (after removing the influence of the SOI) are virtually unchanged and all remain significant at $p < 0.01$, further suggesting that circulation variability associated with the SAM pattern dominates temporal variability in ASL magnitude and Peninsula temperatures during MAM.

Table 2. Seasonal Detrended Partial Correlations over 1979–2015 of Antarctic Peninsula Temperatures with the SOI (After Removing the SAM Index) and the SAM Index (After Removing the SOI)[a]

	DJF		MAM		JJA		SON	
	SOI	SAM	SOI	SAM	SOI	SAM	SOI	SAM
All Peninsula	0.07	0.22	0.04	**0.67***	**0.36**	**0.44***	**0.48***	**0.50***
West	0.07	−**0.32**	**0.28**	**0.48***	**0.43***	0.26	**0.58***	0.25
Northeast	0.02	**0.44***	−0.12	**0.61***	0.23	**0.48***	**0.29**	**0.55***
ASL	−0.26	−**0.76***	−0.23	−**0.48***	−**0.62***	−**0.82***	−0.08	−**0.81***

[a]Also given are detrended partial correlations with ASL magnitude as in Table 1. Statistical significance of partial correlations is denoted as in Table 1.

The ENSO/SAM relationship with western and northeast Peninsula temperatures is investigated spatially in Figures 2 and 3. Similar to Figure 4 of *Ding and Steig* [2013], correlations between Peninsula temperatures and tropical SSTs/500 hPa geopotential height are shown for all seasons (DJF and MAM shown in Figure 2 and JJA and SON shown in Figure 3); however, the western (Figures 2a and 2c and 3a and 3c) and northeast (Figures 2b and 2d and 3b and 3d) Peninsula are investigated separately. The findings of *Ding and Steig* [2013] and results from Table 1 for DJF are confirmed with no significant temporal relationship between tropical SSTs and Peninsula temperatures during DJF. This is possibly due to the strong zonal symmetry of the Southern Hemisphere circulation during DJF [*Karoly*, 1989] manifested as a climatologically weaker ASL in summer [e.g., *Fogt et al*., 2012a; *Turner et al*., 2013b]. It may also be related to the climatologically weaker subtropical jet over the South Pacific sector, weakening anomalous meridional vorticity gradients, and the associated Rossby wave source, thereby weakening the connection between tropical deep convection to the high southern latitudes via poleward propagating Rossby waves [e.g., *Lachlan-Cope and Connolley*, 2006].

The regional circulation anomalies for the western Peninsula during DJF (Figure 2a) show positive pressure anomalies over the Weddell Sea are associated with positive temperature anomalies on the western Peninsula. In contrast, positive temperature anomalies on the northeast Peninsula during DJF (Figure 2b) are associated with positive pressure anomalies north of the Peninsula over the South Atlantic (resembling a positive SAM state). When the positive pressure anomaly east of the Peninsula is located farther poleward over the Weddell Sea, the flow across the Peninsula would be anomalously northeasterly, which would increase poleward heat transport and warm the western Peninsula. When the positive pressure anomaly is located farther equatorward over the South Atlantic, positive zonal wind anomalies would occur across the Peninsula, leading to Föhn effects and adiabatic warming at the northeast Peninsula stations [*Orr et al*., 2008]. It is unclear what the exact influence of the SAM is on the latitudinal position of this regional circulation feature, but there is an indication that positive SAM conditions are associated with a more equatorward positive pressure anomaly over the South Atlantic accompanied with negative pressure anomalies over the Weddell Sea and remaining polar cap, which explains the significant positive correlation between the SAM index and northeast Peninsula stations during DJF.

During MAM, significant tropical Pacific SST correlations are seen for western Peninsula temperatures (Figure 2c) but not for northeast Peninsula temperatures (Figure 2d). A wave train following a great circle out of the western tropical Pacific with a deepened ASL is evident for warm western Peninsula temperatures, but positive SAM-like circulation features are also clearly present outside of the tropics. For the northeast Peninsula, a tropically forced wave train is much less apparent over the South Pacific (i.e., although the correlation values reflect a ridge-trough pattern, it is not as strongly tied to the tropics), and the circulation anomalies over the South Atlantic and Indian Oceans are primarily zonal and SAM-like. The overall weak connection to the tropics and stronger SAM-like circulation features during MAM is consistent with the partial correlations: when local circulation anomalies associated with the SAM are removed, the ENSO correlation with Peninsula temperatures and ASL magnitude becomes much weaker (Table 2).

During JJA and SON (Figure 3), stronger, statistically significant correlations with tropical Pacific SSTs are seen for both western and northeast Peninsula temperatures, consistent with *Ding and Steig* [2013] and correlations seen in Table 1. The circulation anomalies for the western Peninsula appear to be comprised almost entirely of a tropically forced wave train during JJA and SON (Figures 3a and 3c), while the circulation anomalies for the northeast Peninsula (Figures 3b and 3d) still resemble a SAM pattern but with an embedded

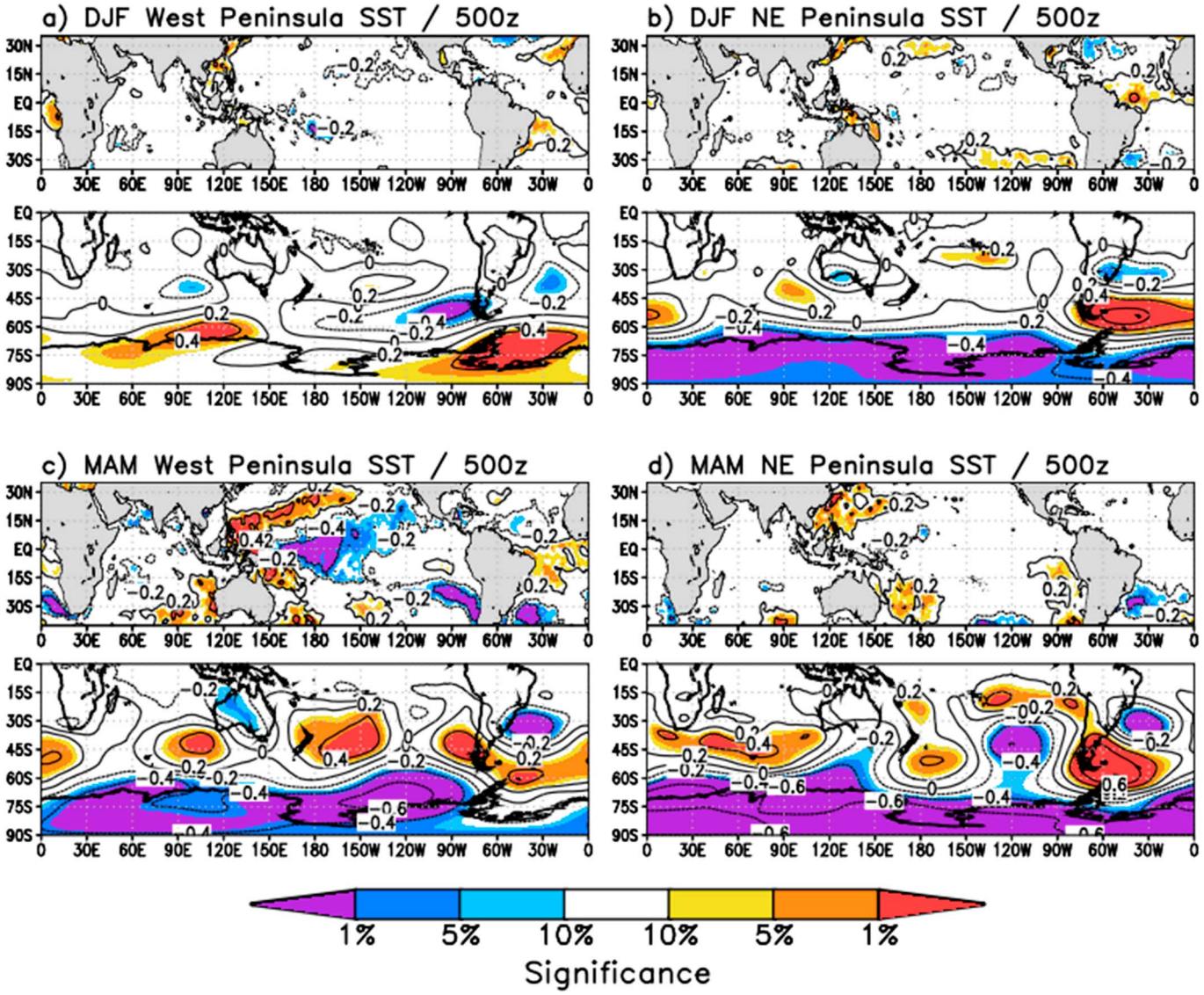

Figure 2. Detrended seasonal correlations of (a and c) western and (b and d) northeast Antarctic Peninsula temperatures with HadISST tropical SST and ERA-Interim 500 hPa geopotential height for (Figures 2a and 2b) DJF and (Figure 2c and 2d) MAM. Correlation coefficients are contoured (contour interval is 0.2, and zero contours are omitted for SST correlations), and statistical significance of correlations at the $p < 0.10$, $p < 0.05$, and $p < 0.01$ is shaded (indicated by reference color bar at the bottom).

tropically forced wave train; this pattern in winter and spring reflects the more zonally asymmetric signature that often characterizes the SAM in these seasons [*Fogt et al.*, 2012b]. Partial correlations with western Peninsula temperatures during JJA and SON confirm a strong tropical connection: after removing the portion of the ENSO correlation related to the SAM, the strength of the ENSO correlation with Peninsula temperatures and ASL magnitude either increases or remains unchanged.

The results presented in Tables 1 and 2 and Figures 2 and 3 are consistent with *Ding and Steig* [2013] in that, there is a very weak tropical connection with Peninsula temperatures during DJF, while strong tropical connections exist during JJA and SON. However, the correlations demonstrate that during MAM, large-scale circulation patterns akin to the SAM are more closely related to interannual Peninsula-wide temperature variability than to circulation patterns associated with ENSO. Additionally, strong SAM features seen during all seasons for the northeast Peninsula may have been overlooked in previous studies. During SON, *Clem and Fogt* [2013] identified a persistent and significant ENSO relationship with western Peninsula temperatures, while the SAM relationship was significant and persistent with northeast Peninsula temperatures. To

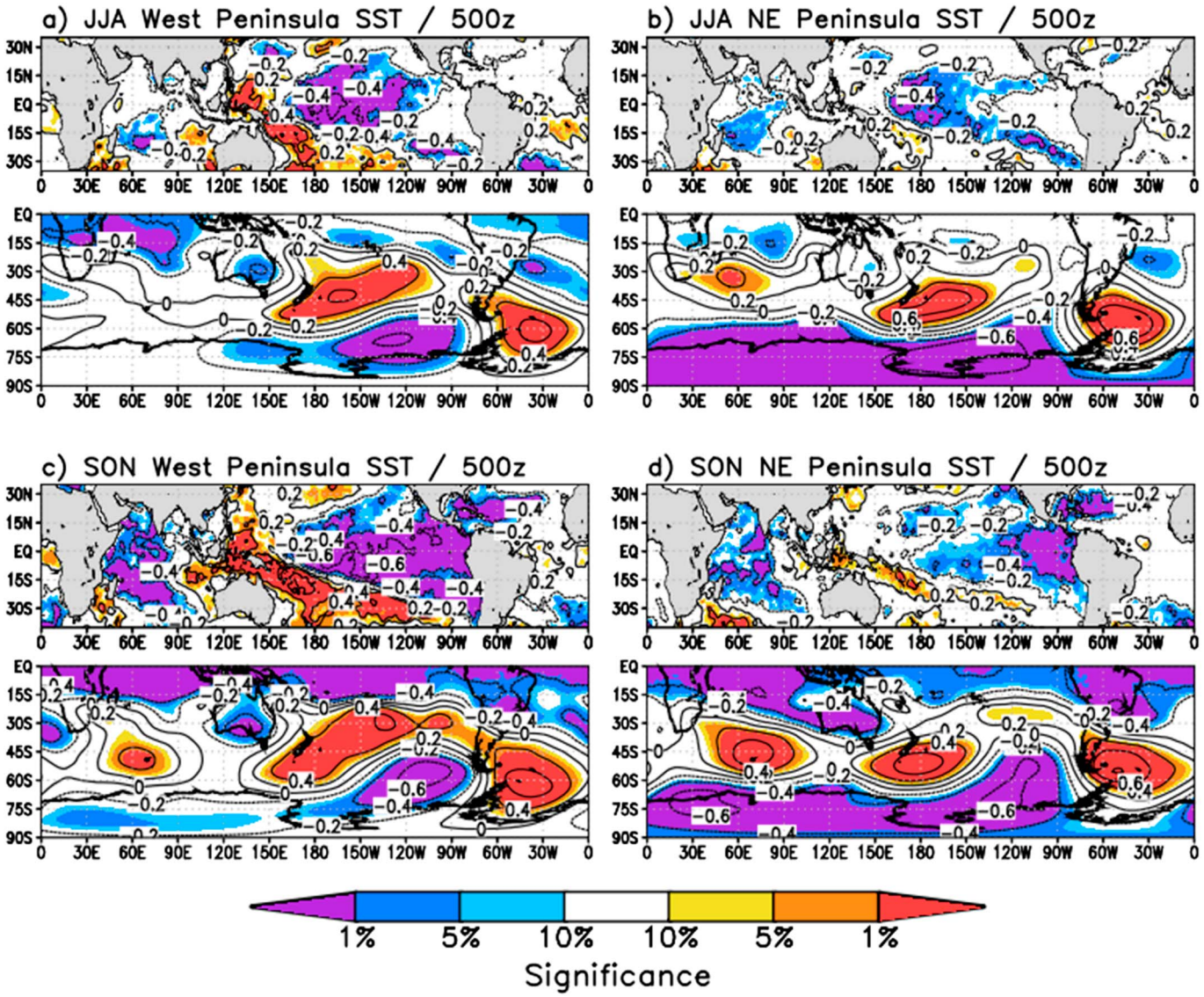

Figure 3. The same as in Figure 2 except for (a and b) JJA and (c and d) SON seasons.

better understand the relative roles of ENSO and SAM on western versus northeast Peninsula climate during MAM and JJA, anomaly composites for each region are investigated.

A list of the six warmest and six coldest years for both regions is shown in Table 3, along with the observed average temperature for the two respective stations and the associated ENSO/SAM phases. The six warmest and coldest years represent the 85th and 15th percentiles of the temperature distribution, respectively, while the ENSO and SAM phases are noted only when the specific index is above its 70th or below the 30th percentile. During DJF, no western Peninsula warm years occurred during positive SAM conditions, and none of the coldest years occurred with negative SAM conditions. Similarly (but opposite in sign), none of the warmest years for the northeast Peninsula occurred with negative SAM conditions, and none of the coldest years occurred during positive SAM conditions. This further supports the significant yet opposing correlation between the SAM index and Peninsula temperatures during DJF. During SON, consistent with the findings of *Clem and Fogt* [2013] for the period of 1979–2012, no warm northeast Peninsula temperature years occurred during negative SAM conditions, and no warm western Peninsula temperature years occurred during El Niño conditions and vice versa. This provides additional evidence confirming the persistent ENSO influence on western Peninsula temperatures and the persistent SAM influence on northeast Peninsula temperatures during SON by expanding the period of analysis to 2015.

Table 3. Top Six Warmest and Coldest Years (Rank Order, 85th and 15th Percentiles, Respectively) by Season for Western and Northeast Peninsula Temperatures Used for Compositing in Figures 4–6[a]

DJF

West Peninsula

Warm Years			Cold Years		
Year	Temp	ENSO-SAM	Year	Temp	ENSO-SAM
1989	1.9	EN	2013	−0.3	neutral
2000	1.7	LN/SAM−	1980	−0.2	neutral
2002	1.5	EN	1999	−0.1	LN/SAM+
2009	1.5	EN/SAM−	1993	0	SAM+
1988	1.4	LN	2015	0	SAM+
1984	1.4	LN/SAM−	2014	0.1	SAM+

Northeast Peninsula

Warm Years			Cold Years		
Year	Temp	ENSO-SAM	Year	Temp	ENSO-SAM
2001	1.6	SAM+	1979	−1.7	EN/SAM−
1994	1.4	EN/SAM+	2000	−1.6	LN/SAM−
1999	1	LN/SAM+	2013	−1.5	neutral
2005	0.9	LN/SAM−	1985	−1.5	SAM−
1992	0.7	EN	2012	−1.4	neutral
1995	0.7	LN	1991	−1.3	SAM−

MAM

West Peninsula

Warm Years			Cold Years		
Year	Temp	ENSO-SAM	Year	Temp	ENSO-SAM
1999	−0.7	LN/SAM+	1980	−6.5	SAM−
2001	−0.8	neutral	1979	−4	neutral
1998	−1.2	EN/SAM+	1992	−4	EN/SAM−
2006	−1.3	LN/SAM+	2002	−4	EN/SAM−
2013	−1.4	LN/SAM+	1981	−3.8	LN/SAM−
2012	−1.5	LN/SAM+	1991	−3.5	EN

Northeast Peninsula

Warm Years			Cold Years		
Year	Temp	ENSO-SAM	Year	Temp	ENSO-SAM
1998	−2.8	EN/SAM+	1990	−12.2	SAM−
1999	−3.3	LN/SAM+	1986	−10.9	SAM−
2006	−4.1	LN/SAM+	1991	−10.9	EN
2000	−4.7	LN/SAM+	1992	−10.8	EN/SAM−
2003	−5.4	SAM+	1987	−10.7	EN/SAM−
1997	−5.4	EN	2007	−10.5	SAM−

JJA

West Peninsula

Warm Years			Cold Years		
Year	Temp	ENSO-SAM	Year	Temp	ENSO-SAM
1989	−3.5	LN/SAM+	1980	−16	neutral
1998	−3.8	LN/SAM+	1987	−14	EN
1983	−4.7	neutral	2015	−11.4	EN/SAM+
2010	−5.5	LN/SAM+	1995	−11.3	SAM−
2000	−5.6	LN	1992	−11.2	EN/SAM−
2003	−5.6	neutral	2002	−10.9	EN

Northeast Peninsula

Warm Years			Cold Years		
Year	Temp	ENSO-SAM	Year	Temp	ENSO-SAM
1989	−6.5	LN/SAM+	2007	−16.9	LN/SAM−
2010	−8.2	LN/SAM+	1980	−16.6	neutral
1985	−9	LN	1995	−16.2	SAM−
1984	−9.4	LN/SAM−	2009	−16.1	EN/SAM−
1983	−9.6	neutral	1986	−15.5	neutral
2000	−9.6	LN	2011	−14.5	LN/SAM−

SON

West Peninsula

Warm Years			Cold Years		
Year	Temp	ENSO-SAM	Year	Temp	ENSO-SAM
2010	−1.8	LN/SAM+	1982	−7.7	EN/SAM−
2008	−1.8	LN/SAM+	1987	−7.5	EN
1989	−2.6	neutral	1980	−7.3	SAM−
1985	−2.6	LN/SAM+	1981	−7.2	neutral
1988	−3.3	LN/SAM−	1986	−6.8	EN/SAM+
2005	−3.4	LN	2013	−6.5	SAM−

Northeast Peninsula

Warm Years			Cold Years		
Year	Temp	ENSO-SAM	Year	Temp	ENSO-SAM
2001	−2.2	SAM+	1997	−9.9	EN/SAM−
2008	−2.5	LN/SAM+	1980	−8.4	SAM−
2010	−2.8	LN/SAM+	1994	−8.3	EN/SAM−
2005	−3.2	LN	2014	−8.3	EN
1985	−3.3	LN/SAM+	2007	−8.1	LN/SAM−
1984	−3.9	LN	2012	−7.8	neutral

[a]Also given is the observed average temperature (°C) for each year and the ENSO/SAM phase. Phases are based on when the climate index (SAM index and either the SOI or Niño 3.4 SST) is above or below the 70th or 30th percentile, respectively. EN = El Niño (negative SOI or positive SST anomaly) and LN = La Niña (positive SOI or negative SST anomaly). Neutral implies that both ENSO and SAM were weak (their indices were between the 30th and 70th percentiles).

During MAM, there is no consistent ENSO phase associated with warm and cold years for either region of the Peninsula (Table 3). The only exception is for cold years on the northeast Peninsula, where no La Niña event was observed, but in MAM the ENSO relationship with northeast Peninsula temperatures on interannual time scales is weak and insignificant (Tables 1 and 2). The SAM phase appears to play a more dominant and consistent role for warm and cold years across both regions of the Peninsula during MAM: the SAM index was never negative during warm years and never positive during cold years across both regions. This is consistent with the significant correlations between the SAM index and all Peninsula temperatures during MAM (Tables 1 and 2).

Anomaly composites for the six warmest years are plotted for MAM (Figure 4) and JJA (Figure 5) only due to analyses already presented here and in previous studies for DJF and SON [e.g., *Ding and Steig*, 2013; *Clem and Fogt*, 2013]. Tropical forcing is investigated using 300 hPa velocity potential and 500 hPa stream function anomalies (Figures 4a–4d and 5a–5d). The extratropical circulation associated with the SAM is investigated using 500 hPa height and 300 hPa wind anomalies (Figures 4e and 4f and 5e and 5f). The local Peninsula low-level circulation is analyzed with 925 hPa meridional temperature advection and wind anomalies (Figures 4g and 4h and 5g and 5h). Anomaly composites using five warmest years as well as the top five and six coldest years were analyzed separately but are not shown. Anomalies for five years show similar results, and the cold years show nearly identical but inverse results.

During MAM (Figure 4) for western Peninsula warm years, a weakly significant, zonally oriented velocity potential couplet is observed over the tropical Pacific, indicating a strengthened Walker circulation commonly observed during La Niña events, consistent with the weak ENSO correlations during MAM. For northeast Peninsula warm years, there are no significant velocity potential anomalies over the tropics, indicating average and/or temporally variable tropical forcing. The 500 hPa stream function anomalies show a tropically forced wave train across the South Pacific and Atlantic for western Peninsula warm years, similar to that seen by *Ding and Steig* [2013], but the circulation anomaly centers, particularly in the vicinity of the ASL, are weak and significant only at $p < 0.10$. Very little in the way of a tropically forced wave train is seen for northeast Peninsula warm years (Figure 4d). Instead, the 500 hPa height and 300 hPa wind anomalies show more of a positive SAM pattern for both regions, with negative height anomalies poleward of ~60°S and positive height anomalies across the middle latitudes. The circulation is marked primarily with meridional wind anomalies for the western Peninsula, including a significantly ($p < 0.05$) deepened ASL and increased northwesterly flow and warm meridional temperature advection just offshore of the western Peninsula (Figures 4e and 4g). The northeast Peninsula warm years show similar circulation features, but the deepened ASL is less marked and the 300 hPa wind anomalies are more zonal across the Peninsula and throughout the South Atlantic and Indian Oceans (Figures 4f and 4h).

The MAM local circulation and meridional temperature advection anomalies for western Peninsula warm years are consistent with previous studies that found meridional wind anomalies to be important for western Peninsula temperatures through modifying local sea ice concentrations and meridional temperature advection [*Ding and Steig*, 2013; *Clem and Renwick*, 2015]. The ENSO and SAM correlations and partial correlations (Tables 2 and 3) show that the SAM index has a significant correlation with ASL magnitude during MAM, while the ENSO correlation with the ASL magnitude is weak and insignificant. Therefore, the correlation between the western Peninsula and the SAM index during MAM is a reflection of the changes in ASL magnitude associated with phases of the SAM, which changes the meridional flow on the western Peninsula. In contrast, zonal wind anomalies, which are closely tied to the phase of the SAM and its degree of zonal symmetry, are more important for the northeast Peninsula. Therefore, it is the changes in the ASL magnitude (and associated meridional flow) and the degree of zonal flow over the Peninsula (particularly related to the pressure pattern over the Atlantic and Indian Oceans downstream) that are the key mechanisms driving the significant SAM index correlation with all Peninsula temperatures during MAM.

For JJA (Figure 5), there is a much clearer tropical connection. For both the western and northeast Peninsula warm years, significant velocity potential anomalies are seen across the tropical Pacific with upward motion/upper level divergence in the western tropical Pacific and subsidence over the central and eastern tropical Pacific. Stream function anomalies at 500 hPa show a clear tropically forced wave train across the South Pacific that terminates over the South Atlantic. The 500 hPa height and 300 hPa wind anomalies primarily indicate a tropically forced wave train (made even clearer in the 500 hPa stream function field) but also weak negative height anomalies over Antarctica reflecting a positive SAM phase. A significantly deepened ASL and associated meridional flow/warm meridional temperature advection anomalies to the Peninsula are also seen during JJA (especially for the western Peninsula). However, the northeast Peninsula warmest years are again associated more with positive zonal wind anomalies across the northeast Peninsula and less related to meridional temperature advection anomalies (Figure 5h) as the ASL is displaced farther westward compared to the western Peninsula warm years (compare Figures 5e and 5f). The tropical connection is also made clear by the ENSO phases associated with warm years, with no El Niño events observed during warm years at either region during JJA. No La Niña events are observed during cold years on the western Peninsula during JJA, indicating that ENSO variability dominates both warm

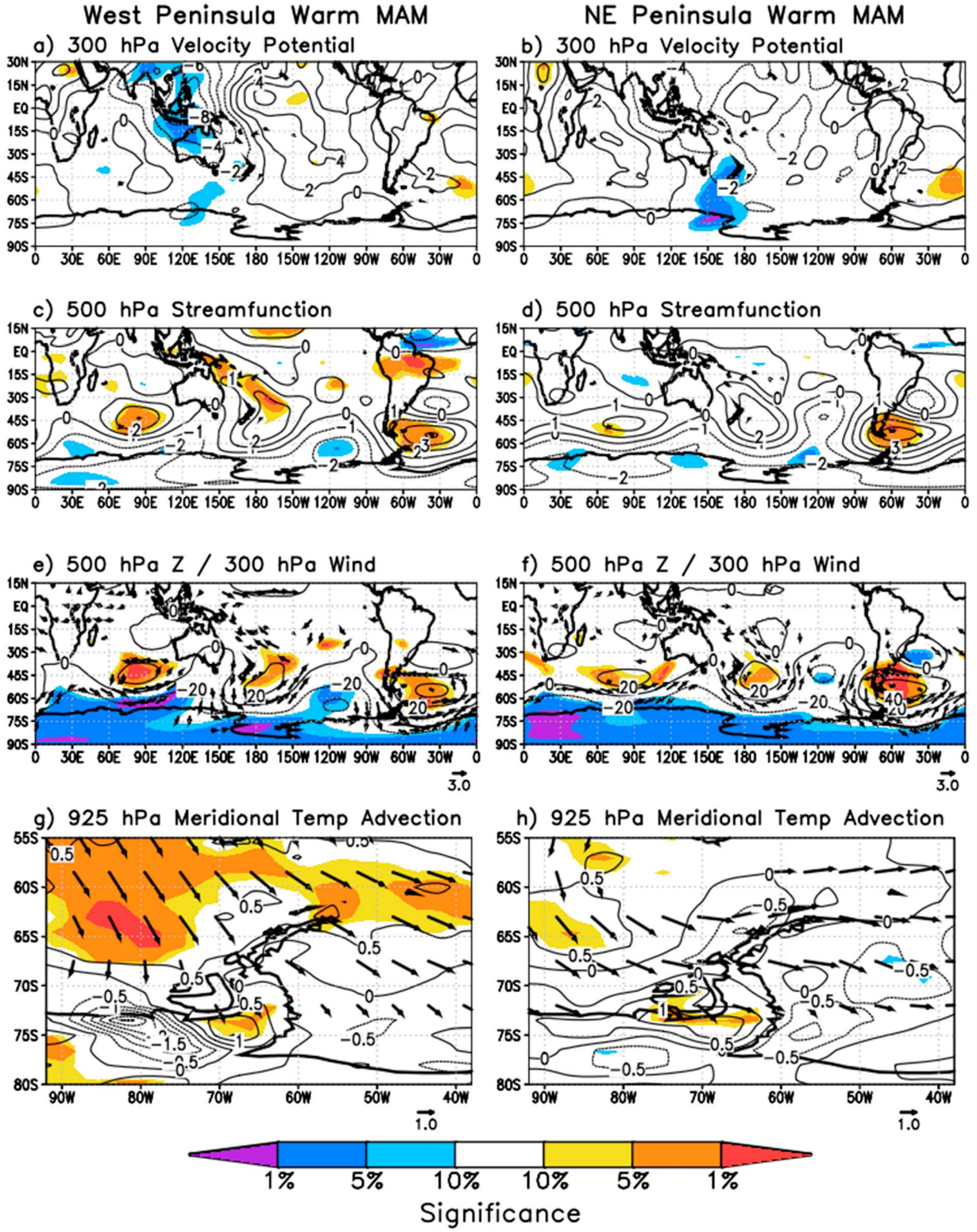

Figure 4. Anomaly composite mean for the six warmest years on the (a, c, e, and g) western and (b, d, f, and h) northeast Peninsula during MAM over 1979–2015. (Figures 4a and 4b) The 300 hPa velocity potential anomalies (contour interval is 2×10^5 m^2 s^{-1}), (Figures 4c and 4d) inverted 500 hPa stream function anomalies (contour interval is 1×10^6 m^2 s^{-1}), (Figures 4e and 4f) 500 hPa geopotential height and 300 hPa wind anomalies (contour interval is 20 m, and wind anomalies are indicated by reference vector in m s^{-1}), and (Figures 4g and 4h) 925 hPa meridional temperature advection ($-v\,\partial T/\partial y$) and 925 hPa wind anomalies (contour interval is 0.5×10^6 °C s^{-1}, and wind anomalies are indicated by reference vector in m s^{-1}). Statistical significance of anomalies is shaded as in Figures 2 and 3. The vectors are plotted only if at least one component of the wind anomaly is significant at the $p < 0.10$ level.

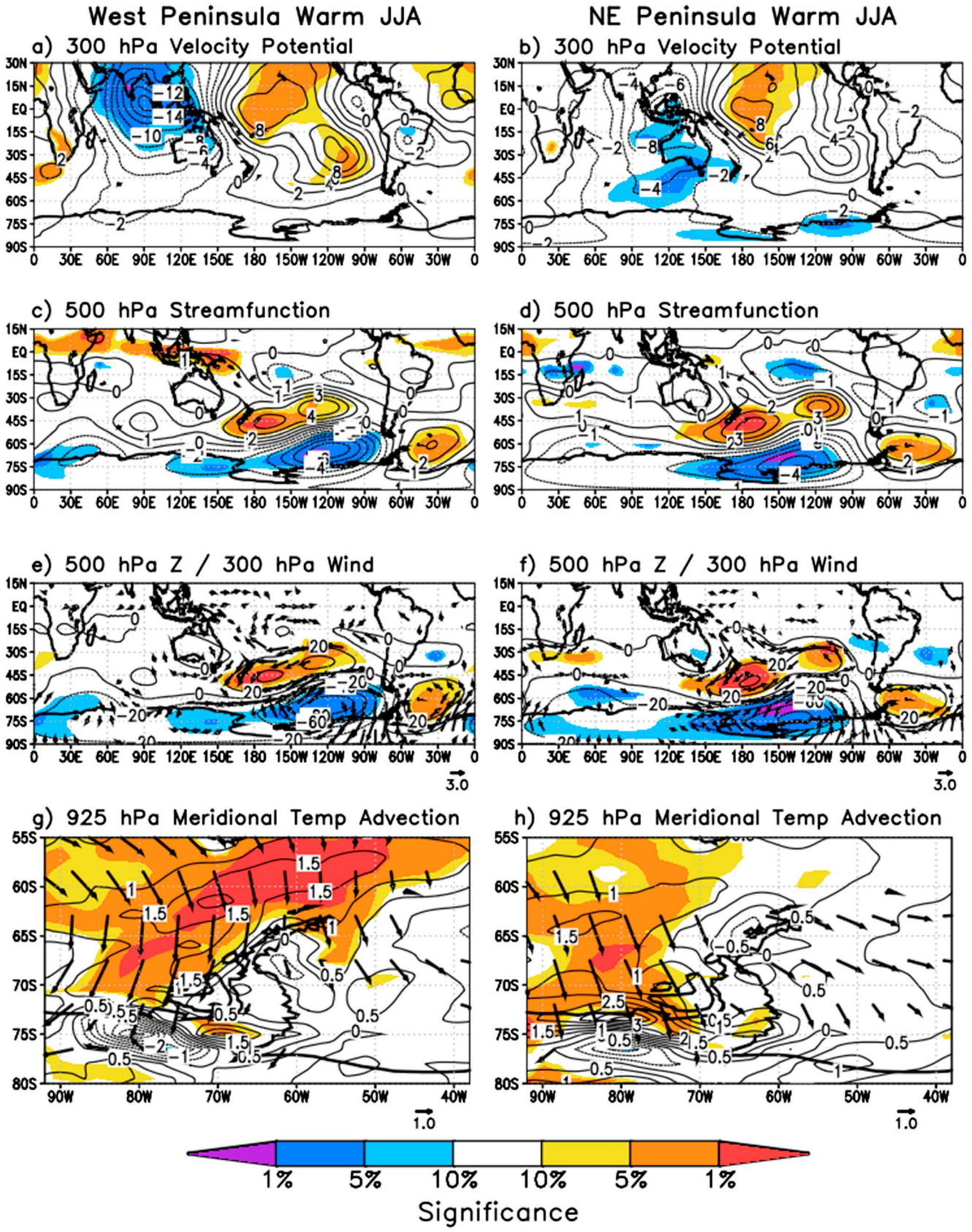

Figure 5. (a–h) The same as in Figure 4 except for the six warmest years during JJA.

and cold years there, while a stronger SAM connection is found for the northeast Peninsula, where no positive SAM years are seen during cold years.

3.2. Regional Circulation Characteristics Across the Peninsula and Their Connection to ENSO and SAM

The regional atmospheric circulation anomalies across the Peninsula (averaged over 64.5–67.5°S) for warm years during all seasons are shown in Figure 6. The years used for compositing are as in Figures 4 and 5 and given in Table 3. Nearly identical, inverse sign anomalies are seen for the six coldest years, and the results shown here (using ERA-Interim at 0.75° latitude-longitude resolution) are qualitatively identical to results using MERRA-2 Reanalysis data and ERA-Interim data at coarser resolutions. The meridional wind anomalies are contoured, and their significance is shaded. Vectors are composed of the zonal wind and (scaled) vertical velocity anomaly, and only vectors with at least one component significant at $p < 0.10$ are shown.

For northeast Peninsula warm years (Figures 6b, 6d, 6f, and 6h), significant westerly flow over the steep Peninsula terrain is clearly seen for all seasons. The flow is primarily westerly during DJF and MAM, where it reaches the steep coastal mountains on the northern Peninsula, ascends over the mountains, and sharply descends on the leeside near Esperanza and Marambio stations and across northern portions of the Larsen Ice Shelf. The same orographic process occurs during JJA and SON, but the low-level flow toward the Peninsula is more northwesterly when taking into account the significant negative meridional component on the eastern side of the Peninsula (shading). *Orr et al*. [2008] demonstrated that flow over the Peninsula during DJF leads to warming on the eastern Peninsula through the Föhn effect. This orographic-driven process is clearly tied to warming on the northeast Peninsula during all seasons, even when the flow is northwesterly. For the western Peninsula warm years (Figures 6a, 6c, 6e, and 6g), meridional flow plays a more important role (meridional wind anomalies are larger in magnitude and generally more significant), and the zonal wind anomalies associated with warm western Peninsula years are too weak to completely cross the Peninsula (there is strong ascent at the coast, but the flow does not crossover to the eastern side).

To identify the relative influence of ENSO and SAM on local winds, partial correlations for the SOI (after removing the SAM index) and SAM index (after removing the SOI) with zonal and meridional winds are plotted in Figures 7 and 8, respectively. Winds at 700 hPa are selected for correlation analysis, as Figure 6 shows the spatial pattern of the zonal and meridional wind anomalies to be well represented at 700 hPa. However, similar results are obtained at all tropospheric levels (10 m above ground level up to 300 hPa) due to the equivalent barotropic nature of the seasonal mean data employed in the correlation maps. The SAM index partial correlation with zonal winds (Figures 7b, 7d, 7f, and 7h) shows strong, statistically significant ($p < 0.01$) positive correlations with zonal winds over the northeast Peninsula during all seasons. This relationship is significant across the entire northern two thirds of the Peninsula during DJF, MAM, and SON, while during JJA a significant correlation is seen only over the northeastern tip of the Peninsula near Esperanza and Marambio stations. In contrast, there is virtually no ENSO relationship with zonal winds over the Peninsula during any season; this is true even when the SAM influence is retained for original SOI correlations (not shown). This confirms and further explains the significant SAM index correlation with the northeast Peninsula during all seasons and the comparatively weaker ENSO correlation; northeast Peninsula temperatures are tied to zonal winds traversing the Peninsula, which is dominated by SAM variability.

Partial correlations with 700 hPa meridional winds are shown in Figure 8. Both the SOI and SAM index exhibit weak correlations with meridional winds during DJF likely due to the highly zonal structure of the Southern Hemisphere circulation and weakened ASL during summer [*Fogt et al*., 2012a, 2012b]. The SOI is weakly correlated with negative (poleward) meridional wind anomalies off the northern tip of the Peninsula and over portions of the northwest Bellingshausen Sea during DJF, while the SAM index exhibits generally weaker, near-zero correlations across the entire Peninsula. The SAM index zero partial correlation line passes between Rothera and Faraday-Vernadsky, with positive correlations to the north and negative correlations to the south. Despite the correlations being very weak, this likely depicts the split flow described by *Orr et al*. [2004] associated with westerly flow encountering the Peninsula and would therefore explain the sign reversal of the SAM index with western Peninsula temperatures during DJF. When the flow over the Bellingshausen Sea toward the Peninsula is primarily zonal (e.g., the flow associated with SAM during DJF), westerly winds may take on a southwesterly component along the northwestern coast as they reach the steep terrain of the Peninsula and the orientation of the northern Peninsula turns easterly. This scenario

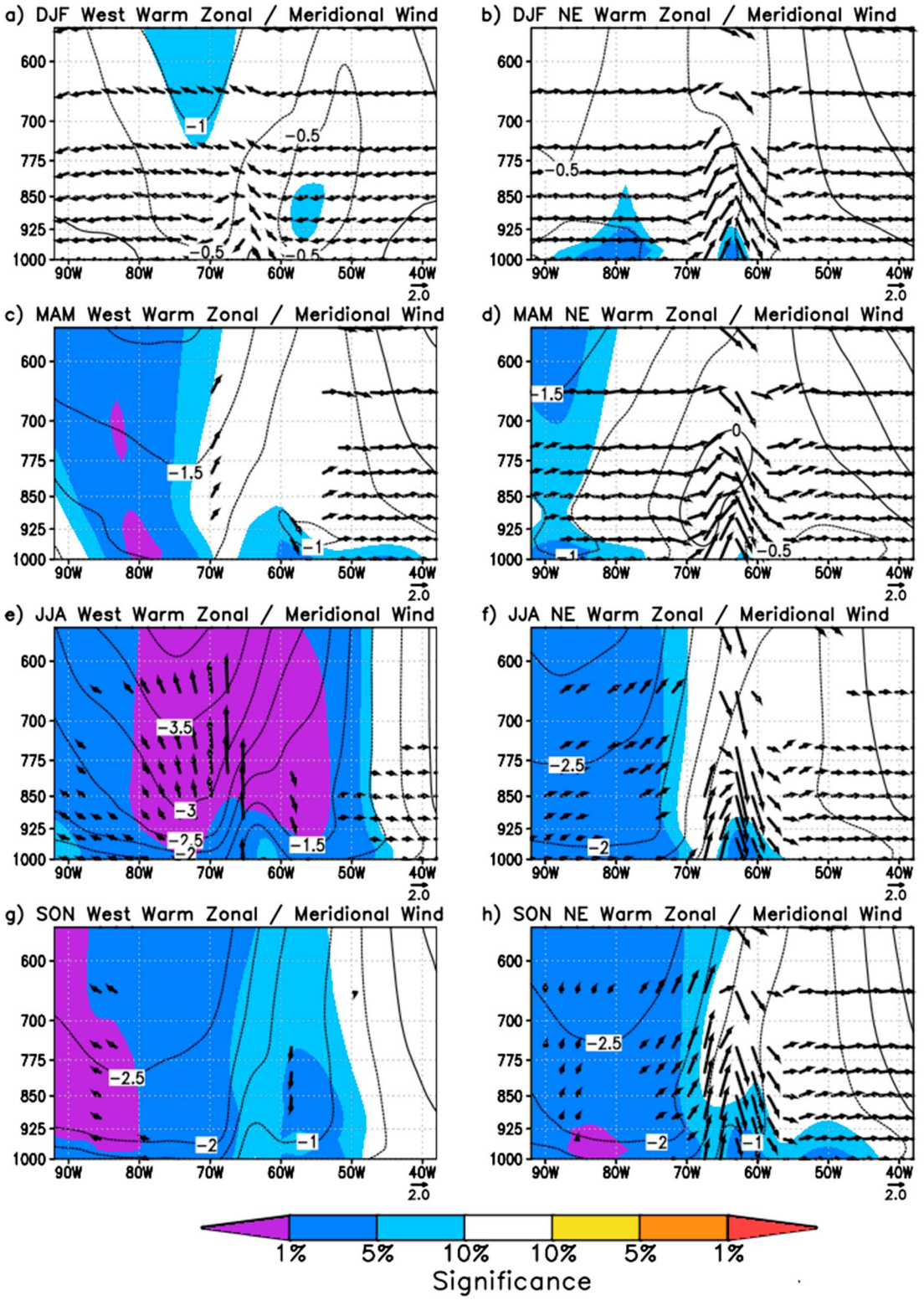

Figure 6. Anomaly composite mean of northern Peninsula (meridionally averaged over 64.5–67.5°S) meridional wind (contours) and zonal vertical circulation (vectors) for the six warmest years on the (a, c, e, and g) western and (b, d, f, and h) northeast Peninsula for (Figures 6a and 6b) DJF, (Figures 6c and 6d) MAM, (Figures 6e and 6f) JJA, and (Figures 6g and 6h) SON. Contour interval for meridional wind anomalies is 0.5 m s^{-1}, and statistical significance of meridional wind anomalies is shaded as in Figures 4 and 5. The vectors are composed of the zonal wind and omega anomalies (scaled -10^2), and the vectors are only plotted if at least component is significant at $p < 0.10$. Wind and omega data are from ERA-Interim employed at 0.75° latitude-longitude resolution. Anomalies and significance are calculated after data are meridionally averaged.

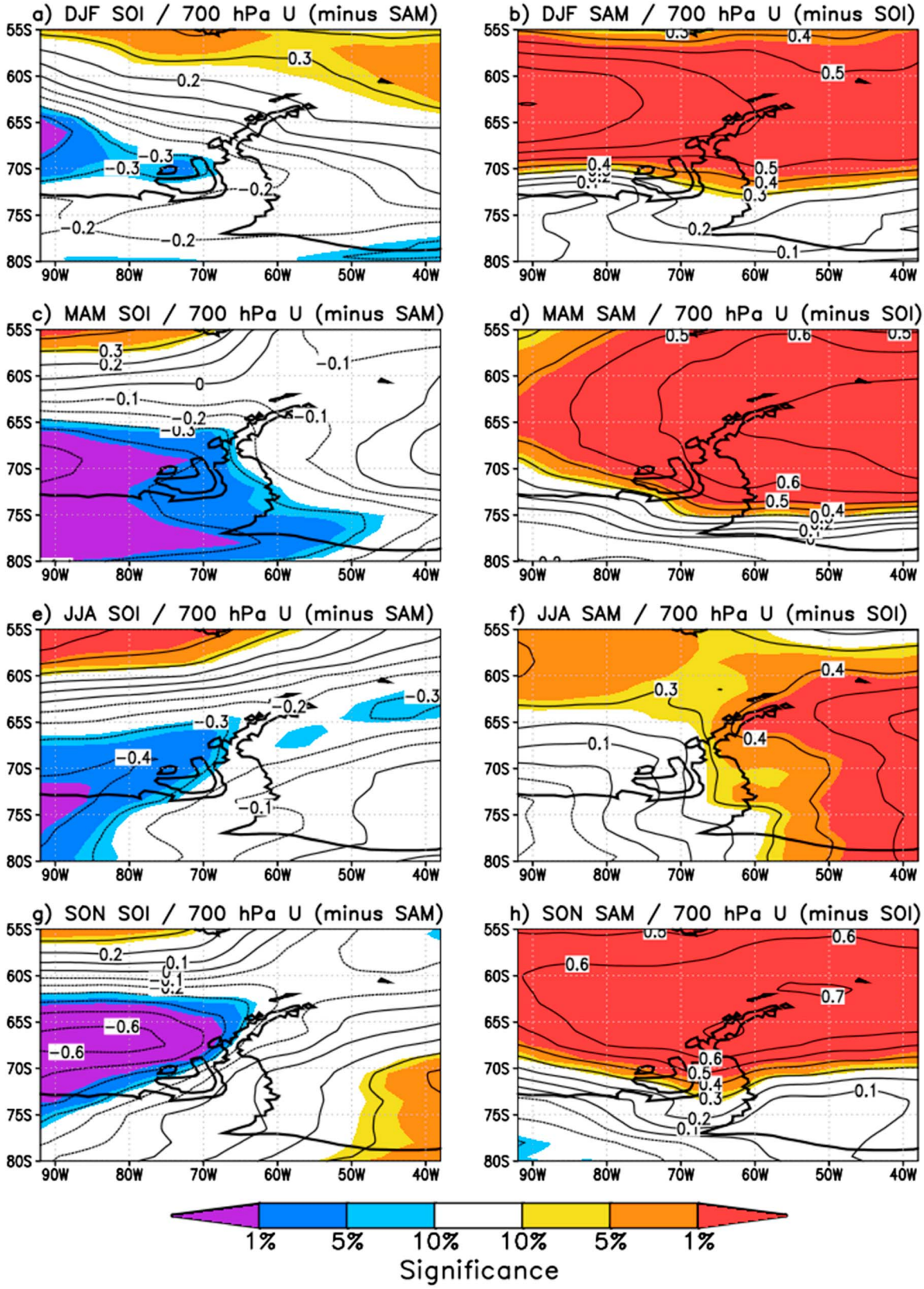

Figure 7. Detrended partial correlations of (a, c, e, and g) SOI (after removing the SAM index) and (b, d, f, and h) SAM index (after removing the SOI) with 700 hPa zonal wind for (Figures 7a and 7b) DJF, (Figures 7c and 7d) MAM, (Figures 7e and 7f) JJA, and (Figures 7g and 7h) SON. Contour interval is 0.1, and statistical significance of correlations is plotted as in Figures 2 and 3.

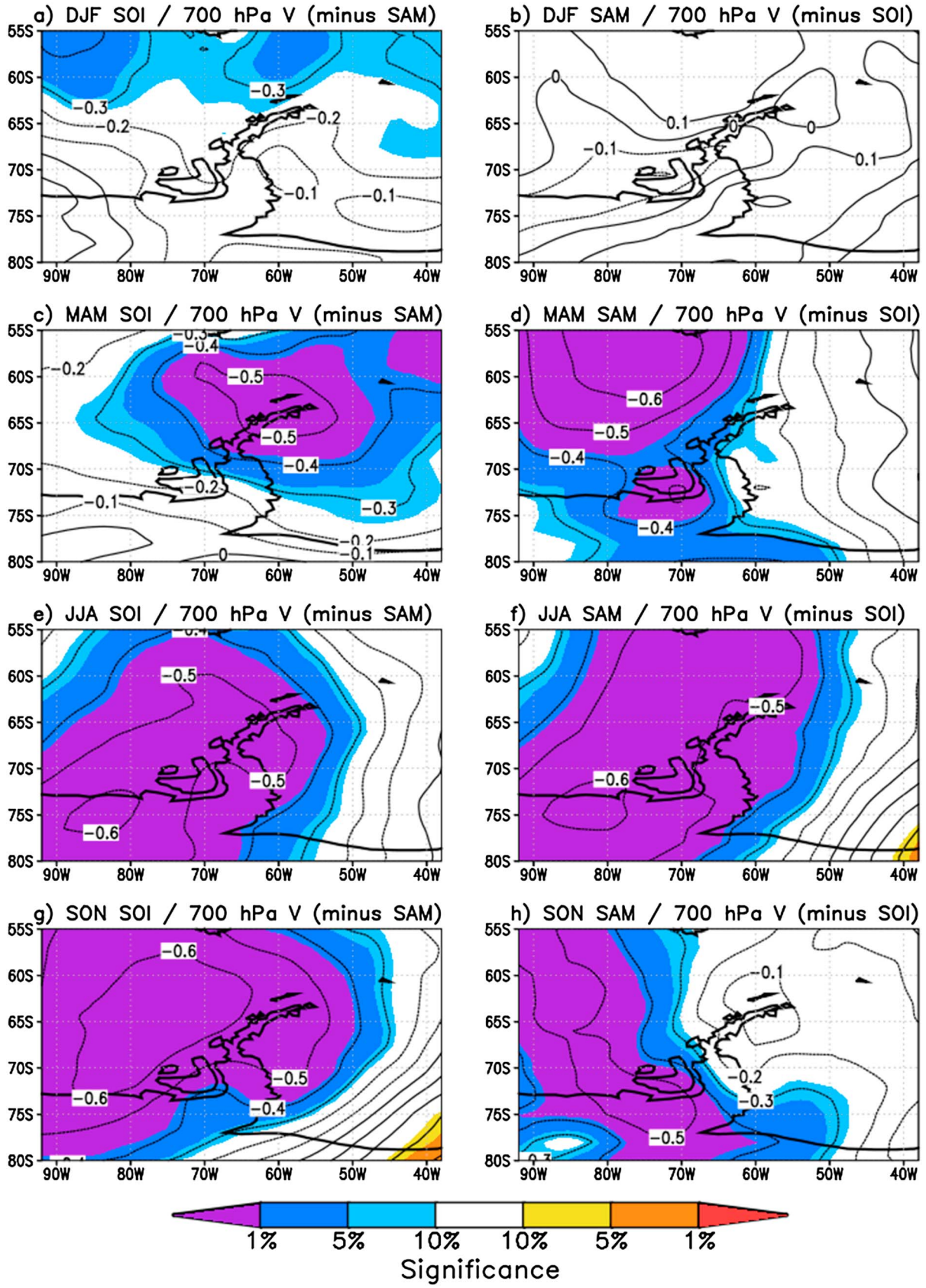

Figure 8. (a–h) The same as in Figure 7 except for 700 hPa meridional wind.

would lead to a slight cooling at Rothera and Faraday-Vernadsky stations. Any remaining sea ice over the Bellingshausen Sea would also be pushed due eastward toward the west Peninsula coast as opposed to southeastward toward the West Antarctic coast which occurs during other seasons.

Outside of DJF, both the SOI and SAM index show significant, same-sign partial correlations across the Peninsula. The winds over the Peninsula related to ENSO are more purely meridional (e.g., there are no significant partial correlations with zonal winds; El Niño is associated with southerly winds, and La Niña is associated with northerly), while the SAM is associated with both meridional and zonal winds outside of DJF (positive SAM is associated with northwesterly winds, and negative SAM is associated with southeasterly winds). The SOI partial correlation with meridional winds is strongest and most widespread during JJA and SON, consistent with the strengthened correlation with Peninsula temperatures and more robust connection to the tropics seen in the JJA composite. During MAM, the SOI partial correlation is significant over a small region on the northwest Peninsula, while the SAM index partial correlation is strongest offshore of the Peninsula over the Bellingshausen Sea stretching poleward toward the southwestern Peninsula/West Antarctic coast. Although speculative, comparing the spatial patterns of the meridional wind partial correlations during MAM, SAM variability potentially has a greater influence on stunting the equatorward sea ice expansion in the southeastern Bellingshausen Sea during MAM (through its impact on the ASL), while meridional wind variability associated with ENSO may play a greater role at bringing warm, northerly flow to the northwest Peninsula.

4. Summary and Conclusions

Results presented in this study indicate there is a spatially and seasonally dependent impact of atmospheric circulation changes associated with ENSO and SAM phases on Antarctica Peninsula temperatures. During DJF, the SAM index is significantly correlated with both western and northeast Peninsula temperatures, but the relationship is of opposite sign between the two locations (positive SAM conditions are associated with warming on the northeast Peninsula and cooling on the western Peninsula). Therefore, when western and northeast Peninsula temperatures are analyzed together, the SAM index correlation appears weak. The cause for the negative correlation between the SAM index and western Peninsula temperatures during DJF appears related to the flow toward the Peninsula (related to SAM variability) being largely zonal during DJF, and as westerly flow (associated with positive SAM conditions) encounters the steep Peninsula topography, it splits bringing a slight southwesterly wind to the northwest Peninsula. However, the exact cause is not fully understood, and higher-resolution dynamical modeling would be helpful to further identify this relationship.

During MAM, we find circulation changes associated with the SAM to explain the majority of Peninsula temperature variability compared to tropical forcing associated with ENSO. Although previous studies have shown that SST *trends* in the tropical Pacific are associated with temperature change on the Peninsula during MAM, we find the relationship with tropical Pacific *variability* on interannual time scales and detrended data to be weak, especially across the northeast Peninsula. Much stronger ENSO-Peninsula temperature relationships are seen during JJA and SON across both sides of the Peninsula.

As shown in *Clem and Fogt* [2013] during SON, there is a spatial dependency of the circulation features associated with ENSO and SAM phases and their resulting impact on Peninsula temperatures. We find the ENSO relationship with Peninsula temperatures to be strongest on the western Peninsula during all seasons outside of DJF, with the overall strength of the relationship being strongest during JJA and SON. Meanwhile, we find a persistent, statistically significant relationship between the SAM index and northeast Peninsula temperatures during all seasons. The SAM-northeast Peninsula relationship exists year-round due to the significant modulation of the zonal wind traversing the northern Peninsula during SAM events. When the SAM is in its positive phase, positive zonal wind anomalies are observed across the northeast Peninsula during all seasons, which brings flow over the Peninsula leading to leeside Föhn winds and adiabatic warming of the northeast Peninsula. This zonal flow is more closely tied to the circulation anomalies over the Atlantic and Indian Oceans, which resemble a more zonally symmetric, positive SAM structure [*Ding et al*., 2012; *Fogt et al*., 2012b]. The ENSO impact on northeast Peninsula temperatures is relatively weaker during all seasons because of its near-zero relationship with the zonal component of the wind over the Peninsula.

Acknowledgments
Three anonymous reviewers are thanked for their helpful comments, which helped clarify our main points. The European Centre for Medium-Range Weather Forecasts (ECMWF) is thanked for providing the ERA-Interim Reanalysis data, which were accessed freely online at http://www.ecmwf.int/en/research/climate-reanalysis. The Global Modeling and Assimilation Office and Goddard Space Flight Center are thanked for providing the MERRA-2 reanalysis data, which were used to confirm results using ERA-Interim. MERRA-2 data were also accessed freely online at http://disc.sci.gsfc.nasa.gov/daac-bin/FTPSubset2.pl. The UK Met Office Hadley Centre is thanked for providing the SST data, which were accessed freely online at http://www.metoffice.gov.uk/hadobs/hadisst/index.html. The NOAA/OAR/ESRL PSD, Boulder, CO, USA, is thanked for providing the ERSST version 4 SST data, which were used to confirm results using HadISST and were accessed freely from their website at http://www.esrl.noaa.gov/psd/. K.R.C. is supported by a Victoria Doctoral Scholarship.

References

Aronson, R. B., et al. (2015), No barrier to emergence of bathyal king crabs on the Antarctic shelf, *Proc. Natl. Acad. Sci. U.S.A.*, *112*(42), 12,997–13,002.

Baines, P. G., and K. Fraedrich (1989), Topographic effects on the mean tropospheric flow patterns around Antarctica, *J. Atmos. Sci.*, *46*, 3401–3415.

Bracegirdle, T. J. (2012), Climatology and recent increase of westerly winds over the Amundsen Sea derived from six reanalyses, *Int. J. Climatol.*, *33*, 843–851.

Bracegirdle, T. J., and G. J. Marshall (2012), The reliability of Antarctic tropospheric pressure and temperature in the latest global reanalyses, *J. Clim.*, *25*, 7138–7146.

Bromwich, D. H., J. P. Nicolas, and A. J. Monaghan (2011), An assessment of precipitation changes over Antarctica and the Southern Ocean since 1989 in contemporary global reanalyses, *J. Clim.*, *24*, 4189–4209.

Clem, K. R., and J. A. Renwick (2015), Austral spring Southern Hemisphere circulation and temperature changes and links to the SPCZ, *J. Clim.*, *28*, 7371–7384.

Clem, K. R., and R. L. Fogt (2013), Varying roles of ENSO and SAM on the Antarctic Peninsula climate in austral spring, *J. Geophys. Res. Atmos.*, *118*, 11, 481–11, 492, doi:10.1002/jgrd.50860.

Clem, K. R., and R. L. Fogt (2015), South Pacific circulation changes and the connection to the tropics and regional Antarctic warming in austral spring, 1979-2012, *J. Geophys. Res. Atmos.*, *120*, 2773–2792, doi:10.1002/2014JD022940.

Dee, D. P., et al. (2011), The ERA-Interim reanalysis: Configuration and performance of the data assimilation system, *Q. J. R. Meteorol. Soc.*, *137*, 553–597.

Ding, Q., and E. J. Steig (2013), Temperature change on the Antarctic Peninsula linked to the tropical Pacific, *J. Clim.*, *26*, 7570–7585, doi:10.1175/JCLI-D-12-00729.1.

Ding, Q., E. J. Steig, D. S. Battisti, and J. M. Wallace (2012), Influence of the tropics on the Southern Annular Mode, *J. Clim.*, *25*, 6330–6348.

Fahnestock, M. A., W. Abdalati, and C. A. Shuman (2002), Long melt seasons on ice shelves of the Antarctic Peninsula: An analysis using satellite-based microwave emission measurements, *Ann. Glaciol.*, *34*, 127–133.

Fogt, R. L., D. H. Bromwich, and K. M. Hines (2011), Understanding the SAM influence on the South Pacific ENSO teleconnection, *Clim. Dyn.*, *36*, 1555–1576.

Fogt, R. L., A. J. Wovrosh, R. A. Langen, and I. Simmonds (2012a), The characteristic variability and connection to the underlying synoptic activity of the Amundsen-Bellingshausen Seas Low, *J. Geophys. Res.*, *117*, D07111, doi:10.1029/2011JD017337.

Fogt, R. L., J. M. Jones, and J. Renwick (2012b), Seasonal zonal asymmetries in the Southern Annular Mode and their impact on regional temperature anomalies, *J. Clim.*, *25*, 6253–6270.

Hosking, J. S., A. Orr, G. J. Marshall, J. Turner, and T. Phillips (2013), The influence of the Amundsen-Bellingshausen Seas Low on the climate of West Antarctica and its representation in coupled climate model simulations, *J. Clim.*, *26*, 6633–6648.

Huang, B., V. F. Banzon, E. Freeman, J. Lawrimore, W. Liu, T. C. Peterson, T. M. Smith, P. W. Thorne, S. D. Woodruff, and H.-M. Zhang (2014), Extended Reconstructed Sea Surface Temperature version 4 (ERSST.v4). Part I: Upgrades and intercomparisons, *J. Clim.*, *28*, 911–930.

Karoly, D. J. (1989), Southern Hemisphere circulation features associated with El Niño–Southern Oscillation events, *J. Clim.*, *2*, 1239–1252.

King, J. C. (1994), Recent climate variability in the vicinity of the Antarctic Peninsula, *Int. J. Climatol.*, *14*, 357–369.

Lachlan-Cope, T. A., W. M. Connolley, and J. Turner (2001), The role of the non-axisymmetric Antarctic orography in forcing the observed pattern of variability of the Antarctic climate, *Geophys. Res. Lett.*, *28*(21), 4111–4114, doi:10.1029/2001GL013465.

Lachlan-Cope, T., and W. Connolley (2006), Teleconnections between the tropical Pacific and the Amundsen-Bellinghausens Sea: Role of the El Niño/Southern Oscillation, *J. Geophys. Res.*, *111*, D23101, doi:10.1029/2005JD006386.

Lefebvre, W., H. Goose, R. Timmermann, and T. Fichefet (2004), Influence of the Southern Annular Mode on the sea ice-ocean system, *J. Geophys. Res.*, *109*, C09005, doi:10.1029/2004JC002403.

Li, X., D. M. Holland, E. P. Gerber, and C. Yoo (2014), Impacts of the north and tropical Atlantic Ocean on the Antarctic Peninsula and sea ice, *Nature*, *505*, 538–542, doi:10.1038/nature12945.

Liu, W., B. Huang, P. W. Thorne, V. F. Banzon, H.-M. Zhang, E. Freeman, J. Lawrimore, T. C. Peterson, T. M. Smith, and S. D. Woodruff (2014), Extended Reconstructed Sea Surface Temperature version 4 (ERSST.v4): Part II. Parametric and structural uncertainty estimations, *J. Clim.*, *28*, 931–951.

Marshall, G. J. (2003), Trends in the Southern Annular Mode from observations and reanalyses, *J. Clim.*, *16*, 4134–4143.

Marshall, G. J., A. Orr, N. P. M. van Lipzig, and J. C. King (2006), The impact of a changing Southern Hemisphere Annular Mode on Antarctic Peninsula summer temperatures, *J. Clim.*, *19*, 5388–5404.

Meredith, M. P., and J. C. King (2005), Rapid climate change in the ocean west of the Antarctic Peninsula during the second half of the 20th century, *Geophys. Res. Lett.*, *32*, L19604, doi:10.1029/2005GL024042.

Orr, A., D. Cresswell, G. J. Marshall, J. C. R. Hunt, J. Sommeria, C. G. Wang, and M. Light (2004), A "low-level" explanation for the recent large warming trend over the western Antarctic Peninsula involving blocked winds and changes in zonal circulation, *Geophys. Res. Lett.*, *31*, L06204, doi:10.1029/2003GL019160.

Orr, A., G. J. Marshall, J. C. R. Hunt, J. Sommeria, C. G. Wang, N. P. M. van Lipzig, D. Cresswell, and J. C. King (2008), Characteristics of summer airflow over the Antarctic Peninsula in response to recent strengthening of westerly circumpolar winds, *J. Atmos. Sci.*, *65*, 1396–1413.

Rayner, N. A., D. E. Parker, E. B. Horton, C. K. Folland, L. V. Alexander, D. P. Rowell, E. C. Kent, and A. Kaplan (2003), Global analyses of sea surface temperature, sea ice, and night marine air temperature since the late nineteenth century, *J. Geophys. Res.*, *108*(D14), 4407, doi:10.1029/2002JD002670.

Rienecker, M. M., et al. (2011), MERRA: NASA's Modern-Era Retrospective Analysis for Research and Applications, *J. Clim.*, *24*, 3624–3648, doi:10.1175/JCLI-D-11-00015.1.

Scambos, T. A., C. Hulbe, M. Fahnestock, and J. Bohlander (2000), The link between climate warming and break-up of ice shelves in the Antarctic Peninsula, *J. Glaciol.*, *46*(154), 516–530.

Scambos, T. A., J. A. Bohlander, C. A. Shuman, and P. Skvarca (2004), Glacier acceleration and thinning after ice shelf collapse in the Larsen B embayment, Antarctica, *Geophys. Res. Lett.*, *31*, L18402, doi:10.1029/2004GL020670.

Simpkins, G. R., S. McGregor, A. S. Taschetto, L. M. Ciasto, and M. H. England (2014), Tropical connections to climatic change in the extratropical Southern Hemisphere: The role of Atlantic SST trends, *J. Clim.*, *27*, 4923–4936.

Skvarca, P., W. Rack, H. Rott, and T. Ibarzábal y Donángelo (1998), Evidence of recent climatic warming on the eastern Antarctic Peninsula, *Ann. Glaciol.*, *27*, 628–632.

Stammerjohn, S. E., D. G. Martinson, R. C. Smith, X. Yuan, and D. Rind (2008), Trends in Antarctic annual sea ice retreat and advance and their relation to El Niño–Southern Oscillation and Southern Annular Mode variability, *J. Geophys. Res.*, *113*, C03S90, doi:10.1029/2007JC004269.

Thompson, D. W. J., J. M. Wallace, and G. C. Hegerl (2000), Annular modes in the extratropical circulation. Part II: Trends, *J. Clim.*, *13*, 1018–1036.

Trivelpiece, W. Z., J. T. Hinke, A. K. Miller, C. S. Reiss, S. G. Trivelpiece, and G. M. Watters (2011), Variability in krill biomass links harvesting and climate warming to penguin population changes in Antarctica, *Proc. Natl. Acad. Sci. U.S.A.*, *108*(18), 7625–7628.

Turner, J., S. R. Colwell, G. J. Marshall, T. A. Lachlan-Cope, A. M. Carleton, P. D. Jones, V. Lagun, P. A. Reid, and S. Iagovkina (2004), The SCAR READER project: Toward a high-quality database of mean Antarctic meteorological observations, *J. Clim.*, *17*, 2890–2898.

Turner, J., S. R. Colwell, G. J. Marshall, T. A. Lachlan-Cope, A. M. Carleton, P. D. Jones, V. Lagun, P. A. Reid, and S. Iagovkina (2005), Antarctic climate change during the last 50 years, *Int. J. Climatol.*, *25*, 279–294.

Turner, J., T. Maksym, T. Phillips, G. J. Marshall, and M. P. Meredith (2013a), The impact of changes in sea ice advance on the large winter warming on the western Antarctic Peninsula, *Int. J. Climatol.*, *33*, 852–861.

Turner, J., T. Phillips, J. S. Hosking, G. J. Marshall, and A. Orr (2013b), The Amundsen Sea Low, *Int. J. Climatol.*, *33*, 1818–1829.

Turner, J., J. S. Hosking, G. J. Marshall, T. Phillips, and T. J. Bracegirdle (2015), Antarctic sea ice increase consistent with intrinsic variability of the Amundsen Sea Low, *Clim. Dyn.*, doi:10.1007/s00382-015-2708-9.

Vaughan, D. G., and C. S. M. Doake (1996), Recent atmospheric warming and retreat of ice shelves on the Antarctic Peninsula, *Nature*, *379*, 328–331.

Vaughan, D. G., G. J. Marshall, W. M. Connolley, J. C. King, and R. Mulvaney (2001), Climate change: Devil in the detail, *Science*, *293*, 1777–1779.

Vaughan, D. G., G. J. Marshall, W. M. Connolley, C. Parkinson, R. Mulvaney, D. A. Hodgson, J. C. King, C. J. Pudsey, and J. Turner (2003), Recent rapid regional climate warming on the Antarctic Peninsula, *Clim. Change*, *60*, 243–274.

Walsh, K. J. E., I. Simmonds, and M. Collier (2000), Sigma-coordinate calculation of topographically forced baroclinicity around Antarctica, *Dyn. Atmos. Oceans*, *33*, 1–29.